Functionalisation of chitosan with methacryloyl and crotonoyl groups as a strategy to enhance its mucoadhesive properties

European Journal of Pharmaceutics and Biopharmaceutics 205 (2024) 114575

Contents lists available at ScienceDirect

European Journal of Pharmaceutics and Biopharmaceutics

journal homepage: www.elsevier.com/locate/ejpb

Functionalisation of chitosan with methacryloyl and crotonoyl groups as a strategy to enhance its mucoadhesive properties

Shiva Vanukuru [a], Fraser Steele [b], Natalia N. Porfiryeva [c], Alejandro Sosnik [c], Vitaliy V. Khutoryanskiy [a,*]

[a] Reading School of Pharmacy, University of Reading, Whiteknights, Reading RG6 6AD, United Kingdom
[b] MC2 Therapeutics, 1A Guildford Business Park Road, Guildford GU2 8XG, United Kingdom
[c] Laboratory of Pharmaceutical Nanomaterials Science, Department of Materials Science and Engineering, Technion – Israel Institute of Technology, Technion City, Haifa 3200003, Israel

ARTICLE INFO

Keywords:
Chitosan
Mucoadhesion
Transmucosal drug delivery
Methacrylic anhydride
Crotonic anhydride
Planaria

ABSTRACT

Mucoadhesive polymers are crucial for prolonging drug retention on mucosal surfaces. This study focuses on synthesising and characterising novel derivatives by reacting chitosan with crotonic and methacrylic anhydrides. The structure of the resulting derivatives was confirmed using proton-nuclear magnetic resonance spectroscopy and Fourier-transform infrared spectroscopy. It was established that the degree of substitution plays a crucial role in the pH-dependent solubility profiles and electrophoretic mobility of the chitosan derivatives. Spray-drying chitosan solutions enabled preparation of microparticles, whose mucoadhesive properties were evaluated using fluorescence flow-through studies and tensile test, demonstrating improved retention on sheep nasal mucosa for modified derivatives. Acute toxicity studies conducted *in vivo* using planaria and *in vitro* using MTT assay with the Caco-2 cell line, a model of the mucosal epithelium *in vitro*, showed that the novel derivatives are not cytotoxic. These findings emphasise the potential of tailored chitosan chemical modifications for enhancing transmucosal drug delivery.

1. Introduction

Adhesion of a dosage form to a mucosal surface is generally referred to as mucoadhesion [1]. Mucoadhesion emerged as a significant concept in the 1980 s, where the adhesion of dosage forms to mucosal surfaces enhanced retention, facilitating drug penetration and improving bioavailability. This development also contributed to advancements in controlled drug delivery systems and localised transmucosal drug delivery. Several established routes for transmucosal drug delivery take advantage of the unique properties of mucosal surfaces, which exhibit common characteristics. These features make them particularly well-suited for mucoadhesive dosage forms, which can prolong residence time at the site of administration and potentially enhance drug absorption [2–4]. Generally, mucoadhesive materials are hydrophilic polymers with the ability to form hydrogen bonds or to interact electrostatically with mucins. For example, chitosan is a well-known cationic polymer which is highly mucoadhesive. It binds to negatively charged mucins on the mucosal membranes [5]. Several theories can elucidate this complex phenomenon, including wetting, diffusion, and electrostatic interactions. Mucoadhesion is likely driven by the simultaneous contributions of multiple factors [6].

Chitosan is a biodegradable cationic biopolymer which is formed when chitin from crustaceans is treated under alkaline conditions. Chitosan has many properties such as wound healing, anti-microbial and anti-fungal effects to make it highly suitable for medical applications [7]. It also has excellent mucoadhesive properties [8,9]. Mucins are glycoproteins present in the mucosal membrane and these are negatively charged due to the sialic acid and sulphate groups present [10,11]. The –OH and $–NH_2$ groups on the chitosan sidechain enable the formation of electrostatic contacts and hydrogen bonds with mucins, enhancing its retention on the mucosa. At acidic pH, protonation of the amino groups on chitosan leads to the polymer becoming positively charged. This cationic nature allows for bonding with negatively charged mucin therefore giving chitosan its mucoadhesive properties [6]. The solubility of chitosan changes with increase in pH of the solution. The amino group becomes deprotonated making the chitosan precipitate out of solution and becoming insoluble at pH > 6–6.5. The limited solubility of chitosan sometimes restricts its applications,

* Corresponding author.
E-mail address: v.khutoryanskiy@reading.ac.uk (V.V. Khutoryanskiy).

https://doi.org/10.1016/j.ejpb.2024.114575
Received 21 August 2024; Received in revised form 18 October 2024; Accepted 4 November 2024
Available online 6 November 2024

sparking strong interest in developing derivatives that exhibit solubility across a broader pH range [12,13].

Chitosan is regarded as a first generation mucoadhesive polymer while some of its derivatives formed by introduction of reactive functional groups to enhance its mucoadhesive properties are classified as second generation mucoadhesive biomaterials. Modification of chitosan is possible primarily because of the presence of the reactive amino and the hydroxyl moieties. Chemically modified derivatives of chitosan are being extensively studied for various activities [14]. Several modifications of chitosan have been reported which attempted to improve its mucoadhesive properties. These include the introduction of thiol groups as reported by Bernkop-Schnürch and co-workers [15]. Our own group demonstrated enhanced mucoadhesive properties of various polymers by introduction of maleimide [16] and methacryloyl groups [17]. Incorporation of these unsaturated groups into the polymer backbone results in a dramatic improvement in their mucoadhesive properties due to the formation of covalent bonds formed with thiols present in the mucins by 1,2-Michael addition reactions [18,19].

Previously, our group reported the functionalisation of chitosan by reaction with methacrylic anhydride to study transmucosal drug delivery on bladder tissue and demonstrated that it has improved solubility and mucoadhesive properties. The methacryloyl groups introduced into the chitosan backbone are known to form covalent bonds with thiols under physiological conditions thereby improving mucoadhesion [20]. To our knowledge, the modification of chitosan by crotonic anhydride has not been previously reported. In this study, we synthesized two types of derivatives by introducing either crotonoyl or methacryloyl groups into chitosan through N-acylation and evaluated how a small difference in the position of the methyl group adjacent to the double bond influences their physicochemical and mucoadhesive properties. The resulting derivatives were fully characterised using Fourier transform-infrared (FTIR) and proton-nuclear magnetic resonance (^{1}H NMR) spectroscopies. Furthermore, these novel derivatives were studied to understand their retention within the ex vivo nasal mucosa by use of tensile test and flow-through wash-off studies. To characterise the toxicological profiles of the novel derivatives, planaria and cell toxicology studies were conducted.

2. Materials and Methods

2.1. Materials

Chitosan of low molecular weight (50,000–190,000 Da; deacetylation degree 20.8 ± 0.5 %), deuterium oxide (D_2O), methacrylic anhydride and crotonic anhydride were obtained from Sigma Aldrich Co., Ltd., Gillingham, UK. Trifluoracetic acid (TFA), sodium hydroxide and acetic acid were provided by Fisher Scientific, Loughborough, UK. The fresh sheep nasal tissues were obtained from PC Turner Abattoir (Farnborough, Hampshire, UK).

For the cell viability, (3-[4,5-dimethylthiazol-2-yl]-2,5 diphenyl tetrazolium bromide) (MTT, Sigma-Aldrich, St. Louis, MO, USA) assay was conducted on the Caco-2 cell line (American Type Culture Collection, ATCC® HTB-37TM, Manassas, VA, USA). To culture this cell line, Dulbecco's Modified Eagle's Medium (DMEM) was purchased from Life Technologies Corp. (Carlsbad, CA, USA) and supplemented with L-glutamine, heat-inactivated fetal bovine serum (FBS) and a combination of penicillin/streptomycin antibiotic mixture (100 units/mL penicillin, 100 μg/mL streptomycin, Sigma-Aldrich).

2.1.1. Purification of methacrylic anhydride and crotonic anhydride

Methacrylic anhydride and crotonic anhydride were purified using vacuum distillation. Methacrylic anhydride was distilled around 87 °C to remove Topanol A inhibitor, while crotonic anhydride was distilled around 125 °C [21].

2.2. Synthesis of chitosan derivatives

Chitosan derivatives were synthesised by adding distilled methacrylic anhydride or crotonic anhydride at three different molar concentrations to 1 % w/v chitosan solution, as reported previously with slight modification [20]. Briefly, 1 % w/v chitosan solution was prepared by dissolving 1 g of chitosan in 100 mL of 3 % acetic acid at room temperature for 12 h (overnight). Then, 0.0025 mol, 0.005 mol and 0.01 mol of crotonic or methacrylic anhydride were added to this solution to produce low, medium, or high crotonoloylated or methacryloylated chitosan. The mixtures were placed in a water bath at 40 °C, shaken at 75 rpm for 12 h. The products were redispersed in deionised water, purified by dialysis with molecular weight cut-off of 12–14 kDa cellulose membrane (Medicell membranes Ltd, London, U.K.) against 4.5 L deionised water with six water changes over 72 h. The final products of the dialysis were placed in the freezer at −20 °C and were finally freeze-dried for 3 – 4 days using Heto PowerDry LL3000 Freeze Dryer (Thermo Fisher Scientific, UK Ltd., Loughborough, UK).

2.3. Characterisation of chitosan derivatives

2.3.1. Proton-Nuclear magnetic resonance spectroscopy

For this, 10–20 mg of the freeze-dried chitosan samples was dissolved in 1 mL of D_2O with 30 μL of TFA. The samples were left overnight at room temperature to fully dissolve. NMR tubes with a 5 mm internal diameter were used to record the spectra for chitosan and its derivatives. ^{1}H NMR spectra were recorded with a Bruker Nanobay 400 MHz two-channel NMR instrument (Bruker UK Ltd., Coventry, UK) and were analysed using MestReNova (Mestrelab Research, Santiago de Compostela, Spain) Version 6.0.2–5475. The spectra were used to determine the degree of substitution.

The degree of substitution (DS) was determined for the derivatives, where all peak integrations were normalised to the peaks in the 3.0–3.8 ppm range, which corresponds to the glucosamine ring of chitosan. The DS was calculated as shown in Eq. (1). Values of 2 and 6 used to divide the peak integrations represent the protons on the substituted moiety and the glucosamine ring of chitosan.

$$\mathrm{DS} = \frac{\text{Integral of protons of subtituted moiety}/2}{\text{Integral of glucosame ring}/6} \times 100\% \quad (1)$$

2.3.2. Fourier-transform infrared spectroscopy

The freeze-dried samples of chitosan and its derivatives were analysed using ATR-FTIR spectroscopy. The samples were scanned with a frequency from 4000 to 600 cm^{-1} with a resolution of 4 cm^{-1}. The data was processed based on an average of 16 scans per spectrum generated by using a Spectrum 100 FTIR Spectrophotometer equipped with an attenuated total reflectance (ATR) accessory (Perkin–Elmer UK Ltd, Buckinghamshire, UK). The data obtained were analysed using Spectrum One software.

2.3.3. Turbidimetric measurements

To understand the effect pH has on the turbidity of chitosan and its derivatives 0.15 % w/v polymer solutions were prepared by dissolving 30 mg of the freeze-dried sample in 20 mL of 3 % acetic acid and left overnight. NaOH solutions were prepared at different molar concentrations of 2, 1, 0.5 and 0.1 M. These were added to the solution in a dropwise manner to increase the pH by capillary action. Turbidity values of the 0.15 % w/v polymer samples were measured at 400 nm with a Jenway 7315 UV–Vis spectrophotometer (Bibby Scientific, Stone, UK).

2.3.4. Electrophoretic mobility

Electrophoretic mobility values of 0.15 % w/v chitosan, methacryloylated and crotonoloylated chitosan solutions were determined in folded DTS-1070 capillary cell using Zetasizer Nano-ZS (Malvern

Instruments, Malvern, UK) at 25 °C. The instrument was operated at a refractive index of 1.37 and an absorbance of 0.01. Triplicate readings were recorded with 30 sub-runs per measurement.

2.3.5. Spray drying

Freeze dried polymers were dissolved in 3 % acetic acid solution to make 1 % w/v polymeric solutions. 0.1 % w/v of sodium fluorescein was added to the solutions and stirred in the dark overnight. The fluorescent solutions were spray dried using a B-290 spray dryer (Büchi Labortechnik AG, Flawil, Switzerland) operated in closed loop mode with a nitrogen atomising gas and nitrogen drying atmosphere as reported by [22]. For every experiment, aspirator was set at 100 % and the inlet temperature was set to 160 °C and experiments were started when the outlet temperature stabilised to 80 °C.

2.3.6. Laser diffraction

Spray dried particles (~20 mg) were dispersed in deionised water (30 mL) and were added to the sample dispersion unit of the Malvern Mastersizer 3000 (Malvern Instruments) dropwise. Chitosan refractive index was set for 1.54 for the samples and all samples had laser obscuration range between 0.5 to 10 %.

2.3.7. Digital microscopy

Spray dried particles were placed on a microscope slide and viewed under VHX – 7000 digital microscope (Keyence Instruments, Hayes, UK) at a magnification of 6000×. Particle size analysis was conducted on the images generated using ImageJ software (National Institutes of Health, Bethesda, MD, USA).

2.4. Ex vivo studies

2.4.1. Artificial nasal fluid preparation

Artificial nasal fluid (ANF) was prepared as reported previously by [23] by dissolving 0.45 g of NaCl, 1.29 g of KCl, and 0.32 g of $CaCl_2{\cdot}2H_2O$ in 1 L of deionised water. All these chemicals were purchased from Sigma Aldrich Co., Ltd., Gillingham, UK. The artificial nasal fluid was kept at 37 ℃ throughout the experiments.

2.4.2. Assessment of mucoadhesive properties using a tensile test

The TA-XT Plus Texture Analyser with an environmental chamber to control temperature (Stable Micro Systems Ltd., Surrey, UK) and a 5 kg load cell was used to study the mucoadhesive properties of all formulations. Sheep nasal tissue was cut into squares of 2 cm × 2 cm and washed with 1 mL of ANF for 1 min before being placed in between rectangular sample holder. The top cover had a circular opening of 25 mm in diameter. The mucosal surface of the tissue was exposed through this opening. The experiments were conducted in an environmental chamber with the temperature controlled at 37.5 °C. Then, 10 mg of spray dried microparticles were attached to the aluminium probe (12 mm in diameter) using a glue dot. Then the probe was lowered, and the table was brought in contact with mucosal tissue. The following test parameters were used: pre-speed test 0.5 mm/s; test speed 0.5 mm/s; post-speed test 1 mm/s; applied force 0.5 N; contact time 60 s; trigger type auto; trigger force auto; and return distance 20 mm as reported previously [17].

2.4.3. Wash-off retention studies

The microparticles of spray dried polymers containing sodium fluoresceine were added to ANF to make 1 mg/mL dispersions. These dispersions were used to study retention as previously reported with a few changes [24]. Briefly, sheep nasal mucosa which is cut 2 cm × 2 cm was mounted onto a glass slide inclined at 45° and placed inside an incubator 37 °C. The tissue was washed with 1 mL of ANF for 1 min to activate mucins. The background fluorescence intensity ($I_{background}$) was collected for a blank tissue. Then 50 μL of the polymeric dispersions were placed on the tissue and fluorescence images were recorded, with initial fluorescence intensity (I_0). After 2 min of dosing, the tissue was washed with ANF using a syringe pump (Harvard Apparatus model 981074, Holliston, MA, USA) at 0.5 mL/min. Fluorescence images of the mucosal tissue (I_t) were collected at pre-determined time points. All images were taken using fluorescence microscope (MZ10F, Leica Microsystems (UK) Ltd., Buckinghamshire, UK) fitted with a DFC3000G digital camera set at 2.5 × magnification, 32 ms exposure time, gamma 1.3 at 527 nm wavelength. The images from each time point were analysed using ImageJ software to measure the fluorescence intensity after each wash. Fluorescence intensity was calculated using Eq. (2)

$$\textit{Fluorescence intensity}(\%) = \frac{I_t - I_{background}}{I_0 - I_{background}} \times 100 \quad (2)$$

The fluorescence intensity at time 0 was set at 100 %. Results are presented as the fluorescence intensity of the spray dried polymers (after subtracting the background fluorescence from each wash image) at different wash-time points as a function of irrigation time (0–120 min). Triplicate experiments were performed for each polymer and values are reported as mean ± standard deviation. The data from wash-off retention studies was analysed to determine how much artificial nasal fluid is required to reduce the fluorescence intensity by half. WO_{50} values of test materials, representing the volume of fluid required to remove 50 % of microparticles from the tissue, were calculated *via* extrapolation of the average wash-off profiles to 50 % using polynomial fitting (5th order) and Wolfram Alpha (a computational knowledge engine) as reported in [25].

2.5. In vivo toxicity

2.5.1. Acute toxicity assay

Schmidtea mediterranea planarian worms were maintained in 10 L of artificial pond water (APW) at room temperature in the dark. They were fed calf liver twice per week, and APW was replaced after each feed. APW was prepared as a mixture of the following salts: 5 M NaCl (3.2 mL), 1 M $CaCl_2$ (10 mL), 1 M $MgSO_4$ (10 mL), 1 M $MgCl_2$ (1 mL) and 1 M KCl (1 mL) and $NaHCO_3$ (1.008 g) in ultra-pure water, with pH adjusted to 7.0. APW was used to dissolve all the test compounds. Chitosan or modified chitosan were dissolved overnight in APW to make 0.1 % w/v solutions after the pH was adjusted to 6, 6.2, 6.4, 6.6, 6.8 with addition of 2 % acetic acid. Chitosan or modified chitosan dissolved in pure APW was used as the control. Planaria (1.0–1.5 cm long) were placed in 24 wells of plate culture (one in each well), and chitosan or modified chitosan solutions were added. Planaria in APW at these pHs were used as control. Acute toxicity tests were run for 24, 48, and 72 h and the number of live/dead planaria was recorded. Planaria that did not move after agitation were considered dead. Experiments were performed as triplicate for each polymer solution at each pH.

2.5.2. Planaria toxicity fluorescent assay

The experiment was slightly modified from the procedure previously developed by our group [26]. Following a 24-h treatment with 0.1 % of the test substances (unmodified chitosan and modified derivatives) at different pH conditions, the planaria were exposed for 1 min to a 0.1 % w/v sodium fluorescein solution in water in APW. The excess fluorescein solution was then removed from the planaria by immersing them in APW for 15 min. Each worm was placed on a microscopy glass slide and then immobilised with a few drops of a 2.0 % w/v type A gelatin solution (Sigma-Aldrich). The microscopy glass slide was placed on level surface of ice flakes (−0.5 °C to −0.8 °C) until the gel hardened. Fluorescence photos of the worms were captured using a Leica MZ10F stereomicroscope (Leica Microsystems (UK) Ltd.) fitted with a DFC3000G digital camera set at 2.0 × magnification, 160 ms exposure time, and gamma 0.7. The images from each planaria were analysed using ImageJ software to measure the pixel intensity. Triplicate experiments were performed for each polymer at each pH and values are reported as mean fluorescence intensity ± standard deviation.

2.6. Cell viability of chitosan derivatives

The effect of the chitosan and its derivatives on cell viability was determined using the MTT assay using the Caco-2 cell line cultured in DMEM (see above) under humidified conditions with a 5 % CO_2 atmosphere at 37 °C and cells were split every 4–5 days. Caco-2 cells were harvested using trypsin-EDTA (0.25 % w/v, Sigma-Aldrich). The quantification of the living cells was carried out by the trypan blue exclusion assay (0.4 % w/v, Alfa Aesar, Heysham, UK). For the assay, Caco-2 cells were cultured in 96-well plates (20×10^3 cells/well) and allowed to attach for 24 h at 37 °C. Subsequently, the medium was removed, and 180 μL of the new medium, along with 20 μL of chitosan and its derivatives, was added (final concentrations of 0.01, 0.05, and 0.1 mg/mL). To achieve this, the stock polymer solution (1 mg/mL) was adjusted to a pH of 6.5, and then underwent sterilisation through filtration (0.22 μm syringe filters, Merck Millipore Ltd., Dublin, Ireland). The solution was dissolved in the medium to prepare concentrations of 0.5 and 0.1 mg/mL. Following incubation periods of 4 and 24 h, the medium was replaced with fresh medium (100 μL) and MTT solution (25 μL, 5 mg/mL, EMD Millipore Corp., Burlington, MA, USA) and left for an additional 3 h of incubation. Then, the medium was discarded, and insoluble formazan crystals were dissolved using 100 μL of dimethyl sulfoxide (DMSO, CARLO ERBA Reagents GmbH, Emmendingen, Germany). The absorbance was read using a Multiskan GO Microplate Spectrophotometer (Thermo Fisher Scientific Oy, Vantaa, Finland) equipped with Skanlt™ Software for Microplates Readers (Thermo Fisher Scientific) at 530 nm. Untreated cells in the medium were used as controls and considered 100 % viable.

2.7. Statistical evaluation

One-way ANOVA test with 95 % confidence interval as the minimal level of significance was employed as the statistical tool to evaluate the data.

3. Results and discussion

Crotonoloylated and methacryloylated chitosan were synthesised by reacting chitosan with crotonic and methacrylic anhydrides via single step N-acylation reaction as shown by the reaction scheme in Fig. 1. Six different derivatives were synthesised with three different molar concentrations of the anhydrides (Table 1).

3.1. ^1H NMR spectroscopy

^1H NMR spectroscopy is a very useful technique that could provide both qualitative and quantitative information about the chemical modification of chitosan. In our previous study as reported in [20], we detailed the synthesis of methacrylated chitosan using methacrylic anhydride without its prior purification. The ^1H NMR of the chitosan derivatives did include some signals at around 1.5 to 1 ppm that belonged to Topanol A as a stabilising additive. Similar signals are present in the spectra of chitosan derivatives synthesised in this study (**Figure S1**). To prepare chitosan derivatives of better purity, in this study methacrylic and crotonic anhydrides were then additionally purified by distillation prior to their reaction with chitosan. Fig. 2a and b show the ^1H NMR spectra of chitosan and its derivatives recorded in D_2O containing TFA. The ^1H NMR spectrum of chitosan has two characteristic signals. Firstly, the signal associated with the $–CH_3$ protons of the acetylated groups at around $\delta = 1.8$ ppm. The glucosamine ring of chitosan has broad signals which are found between $\delta = 3–3.8$ ppm [27]. All the spectra of chitosan and its derivatives have these signals as well. There are two additional peaks found in the spectra of the crotonoloylated derivatives around $\delta =$ 6.0 ppm and 6.8 ppm associated with the protons of C = C in the

Table 1
Parameters of synthesis.

Parameters	Crot-Chi $_{Low}$	Crot-Chi Medium	Crot-Chi High	Meth-Chi $_{Low}$	Meth-Chi Medium	Meth-Chi High
Mass of chitosan (g)	1	1	1	1	1	1
Moles of anhydride added	0.0025	0.005	0.01	0.0025	0.05	0.01
Volume of anhydride added to chitosan solution (mL)	0.371	0.741	1.482	0.372	0.745	1.489

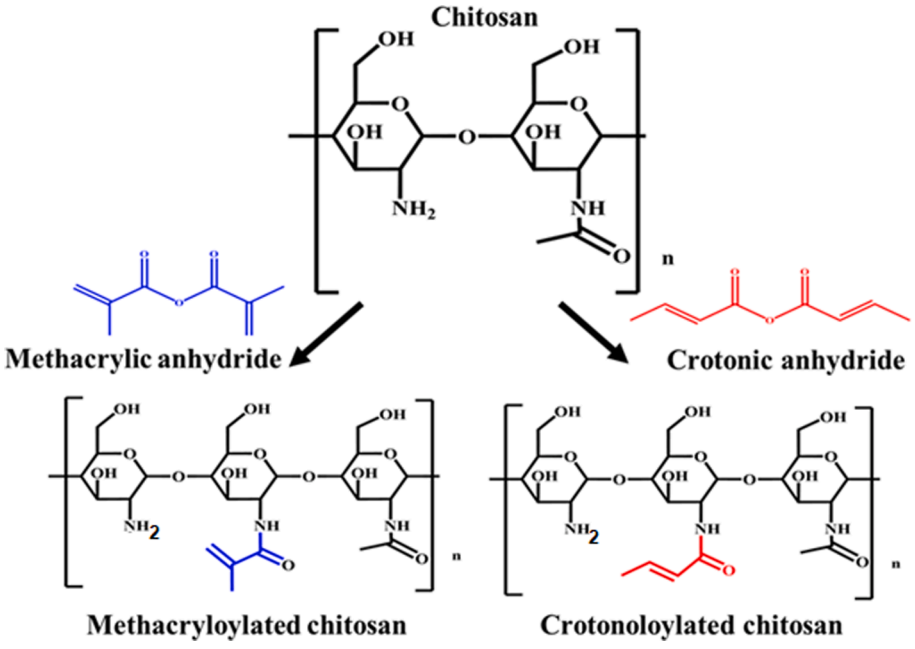

Fig. 1. Reaction scheme for the synthesis of crotonoloylated and methacryloylated chitosan derivatives.

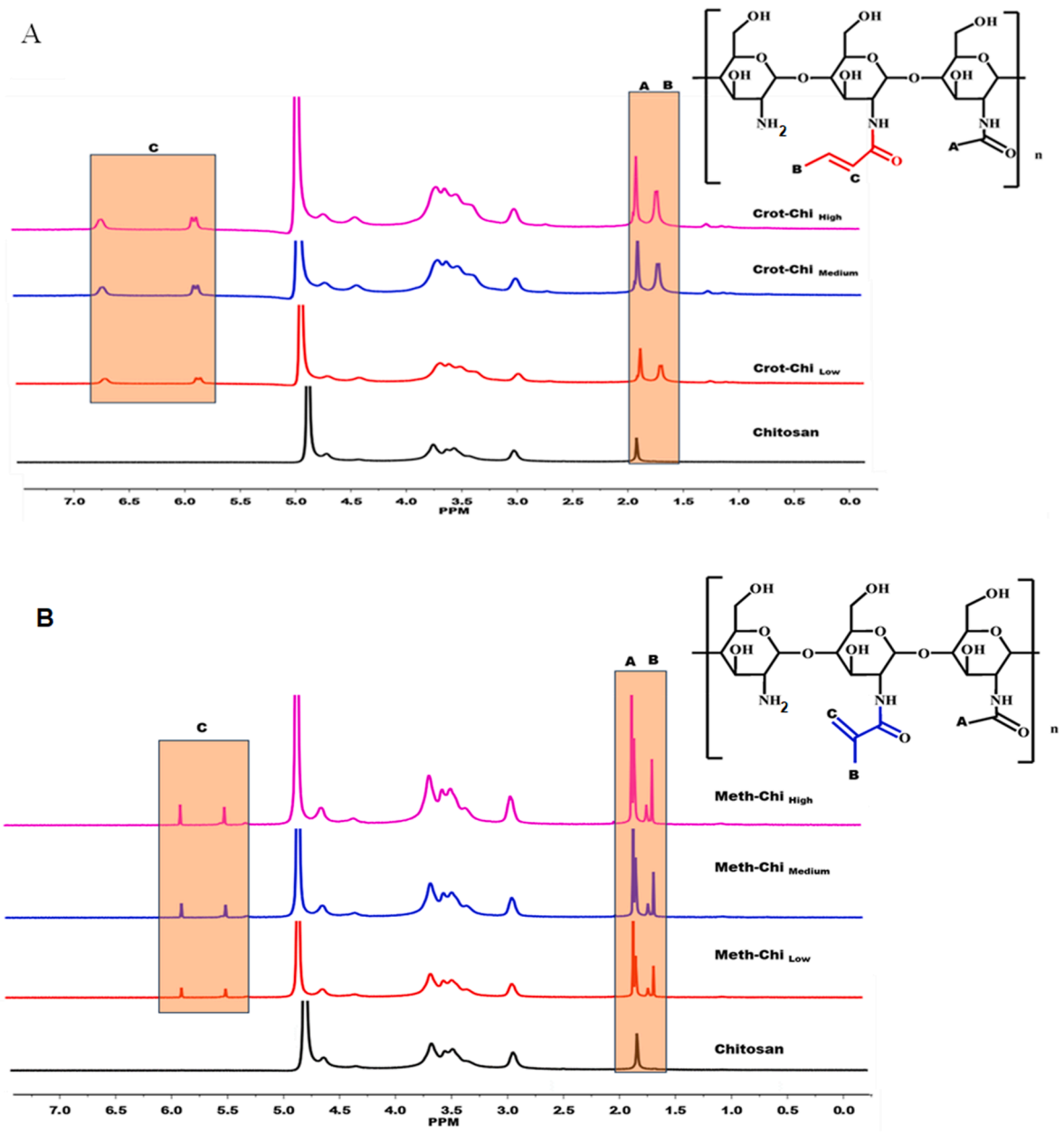

Fig. 2. ^{1}H NMR spectra of parent chitosan and its crotonoloylated derivatives (A) and of (B) parent chitosan and its methacryloylated derivatives in D_2O containing TFA.

crotonoyl moiety conjugated to chitosan. However, the spectra of crotonoloylated derivatives have a downfield shift in comparison to crotonic anhydride which has these signals at $\delta = 5.8$ and 6.6 ppm. For the methacryloylated derivatives (Fig. 2b) additional signals are evident at $\delta = 5.5$ ppm and 6.0 ppm responsible for the protons of alkenyl double bond in the methacryloyl groups conjugated to chitosan [28]. Also, the additional methylene signal at around $\delta = 1.6$ ppm appeared in the spectra of both derivatives due to the protons of $-CH_3$ associated with crotonoloyl and methacryloyl moieties [29].

3.2. FTIR spectroscopy

FTIR analysis was carried out as a qualitative technique to further confirm the successful derivatisation of chitosan (Fig. 3). The sharp absorption bands found at 1028 and 1150 cm^{-1} are associated with the glucosamine ring of chitosan; these represent the vibrations of C–C and C-O bonds [30]. Since chitosan used in this study is not completely deacetylated, the band found around 1377 cm^{-1} corresponds to the acetamide group. The band found at 1557 cm^{-1} corresponds to the N–H bond associated with the amine groups. The –CH groups stretching is visible at around 2800–2900 cm^{-1}, and the O–H stretching is represented by a broad band at 3360 cm^{-1}. There are many absorption bands which are the same between chitosan and its derivatives with the major difference being the appearance of additional bands between 1626 and 1654 cm^{-1}. These bands represent the alkenyl C=C bond stretch and an amide C=O stretch confirming the successful conjugation of crotonoloyl and methacryloyl groups into chitosan. Furthermore, the sharper band at 2900 cm^{-1} is likely responsible for C=C–H alkyl stretch due to the presence of crotonoyl and methacryloyl groups in the chitosan derivatives [31–33].

3.3. Quantification of the degree of substitution

DS was calculated using ^{1}H NMR spectral data. For this, the mean

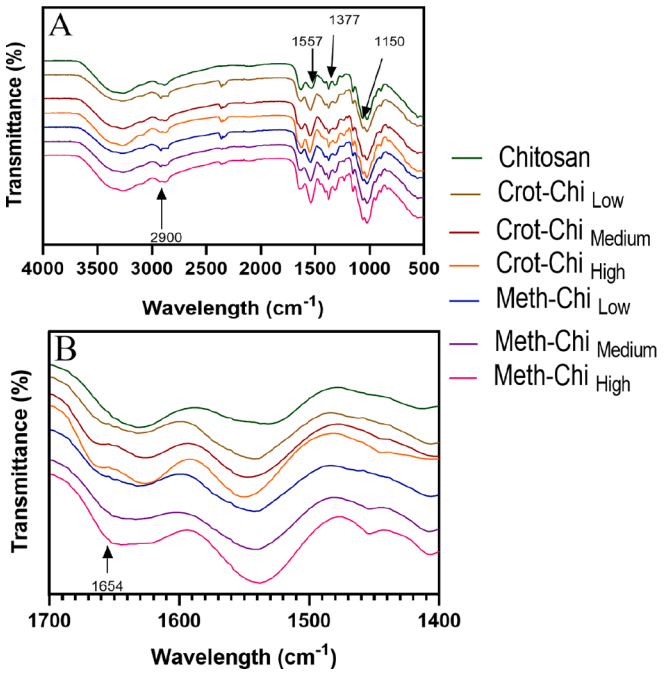

Fig. 3. FTIR spectra of chitosan, its crotonoloylated and methacryloylated derivatives between 600 cm^{-1} to 4000 cm^{-1} (A) and between 1600 and 1700 cm^{-} (B).

intensity of the substituted moiety to that of the glucosamine protons (δ = 3–3.8 ppm) was used to calculate the DS, as previously reported [20]. Results are summarised in Table 2.

3.4. Turbidity and electrophoretic mobility measurements

It is well known that chitosan is soluble under acidic conditions; it becomes insoluble at pH values >6.5 [12]. The degree of acetylation of chitosan has a strong influence on its solubility in water. Additionally, the molecular weight of chitosan determines its solubility profile with low molecular weight chitosan being more soluble compared to high molecular weight derivatives [13]. Fig. 4a and b show the dependence of turbidity of chitosan and its derivatives on the solution pH. It is clearly seen that the solution of parent (unmodified) chitosan becomes turbid at around pH 7. This is in good agreement with the previous reports [12]. The crotonoylated and methacryloylated derivatives of chitosan show distinctly different turbidity–pH profiles. Methacryloylated chitosan samples at low and medium degrees of substitution (8.4 % and 18.5 %) exhibit a pH-dependent solubility like the parent chitosan, with a sharp increase in turbidity observed at slightly higher pH values (Fig. 4b). The chitosan solution, with a high degree of methacryloylation (24.9 %), maintains a slight turbidity across all measured pH conditions, with a subtle rise in turbidity noted as the pH increases. The turbidity–pH profiles of all crotonoloylated derivatives are substantially different compared to the parent chitosan. Fig. 4a shows that the water solubility of crotonoloylated chitosan with the degree of substitution of 18.1 % (Crot-Chi_{Low}) is pH dependent though turbidity is observed only at pH values >9.5. The derivatives with the degrees of crotonoylation of 26.1 % and 37.3 % (Crot-Chi_{Medium} and Crot-Chi_{High}, respectively) remain slightly turbid in the pH range studied and show very little dependence on the solution pH. The influence of pH on the solubility of chitosan and its derivatives is governed by multiple factors. First, the solubility of chitosan is known to be affected by its crystallinity. The intra- and intermolecular hydrogen bonding in chitosan makes it a semi-crystalline polymer, which limits its aqueous solubility. Disrupting the crystalline structure allows for an increase in the solubility of chitosan. When N-acylation occurs the disruption of the crystalline structure owing to the more limited ability to form hydrogen bond bridges changes the pH dependence of the solution turbidity. Methacryloylated chitosan derivatives with relatively low degrees of substitution (8.4 % and 18.5 %) have broader solubility window compared to unmodified chitosan. This is likely due to the partial disruption of semi-crystalline nature of chitosan caused by introduction of small number of bulky methacryloyl groups [12].

Compared to low and medium methacryloylated chitosan derivatives which did have a turbidity increase at pH > 7, medium and high modified crotonoloylated chitosan samples and high modified methacryloylated chitosan sample formed slightly turbid colloidal suspensions even at low pH values. This is likely to be due to the slightly hydrophobic nature of methacryloyl and crotonoyl groups that cause the aggregation of the macromolecules in aqueous medium [20].

Electrophoretic mobility data of chitosan and its crotonoloylated and methacryloylated derivatives are shown in Fig. 4C and D. This physical parameter refers to the velocity of the charged particles in presence of an electric field. Chitosan is a cationic polymer, where the protonation of its amino groups allows it to dissolve in acidic media. Consequently, parent chitosan exhibits maximum electrophoretic mobility at lower pH levels due to the increased positive charge from protonation. Modifying the chitosan with bulky methacryloyl and crotonoyl groups via N-acylation reduces its net positive charge. The charge diminished as more of the amino groups were modified with an increase in the degree of substitution. Additionally, an increase in pH also decreases the charge due to the deprotonation of amino groups. At higher pH values, the electrophoretic mobility values go below zero; this could be explained by formation of insoluble particles at pH > 7 with contributions from excessive OH^{-} ions present due to addition of NaOH to the polymeric solutions [34–36]. The derivatives of chitosan show a tendency to reach negative electrophoretic mobility values at slightly lower pHs.

Table 2
Calculation of degree of crotonoloylation and methacryloylation from ^{1}H NMR integration results.

Sample	Integral of substituted moiety/2	Integral of glucosamine proton/6	DS (%)
Crot-Chi_{Low}	0.03	0.17	18.1
Crot-Chi_{Medium}	0.79	3.03	26.1
Crot-Chi_{High}	0.72	1.93	37.3
Meth-Chi_{Low}	1.01	11.98	8.4
Meth-Chi_{Medium}	1.01	5.46	18.5
Meth-Chi_{High}	1.02	4.08	24.9

3.5. Preparation of spray-dried particles and their characterization

Currently there are drugs on the market which are nasally administered. Nasal drug delivery is mostly used to treat conventional areas of upper respiratory tract infections or for the treatment of localised diseases related to the nose. However, there has been an increasing interest in nasal drug delivery to treat systemic conditions as well as neurodegenerative conditions [37,38]. The direct access available from the olfactory region and trigeminal nerves to the central nervous system (CNS) has made intranasal drug delivery a rapidly expanding area. The advantage of nasal drug delivery to target the CNS diseases while circumventing the problem of blood brain barrier (BBB) increased the interest in nasal drug delivery. The other advantages include bypassing the first pass metabolism which occurs with oral drug administration. However, the main challenge for nasal drug delivery is the insufficient drug absorption, which is a problem due to mucociliary clearance and short retention time in the nasal pathway [39–41]. Currently, there are around 25 drugs within UK licenced for intranasal drug delivery, most of these are formulated as sprays with a few formulated as ointments and drops. Particle size of formulations is a key criterion for nasal deposition.

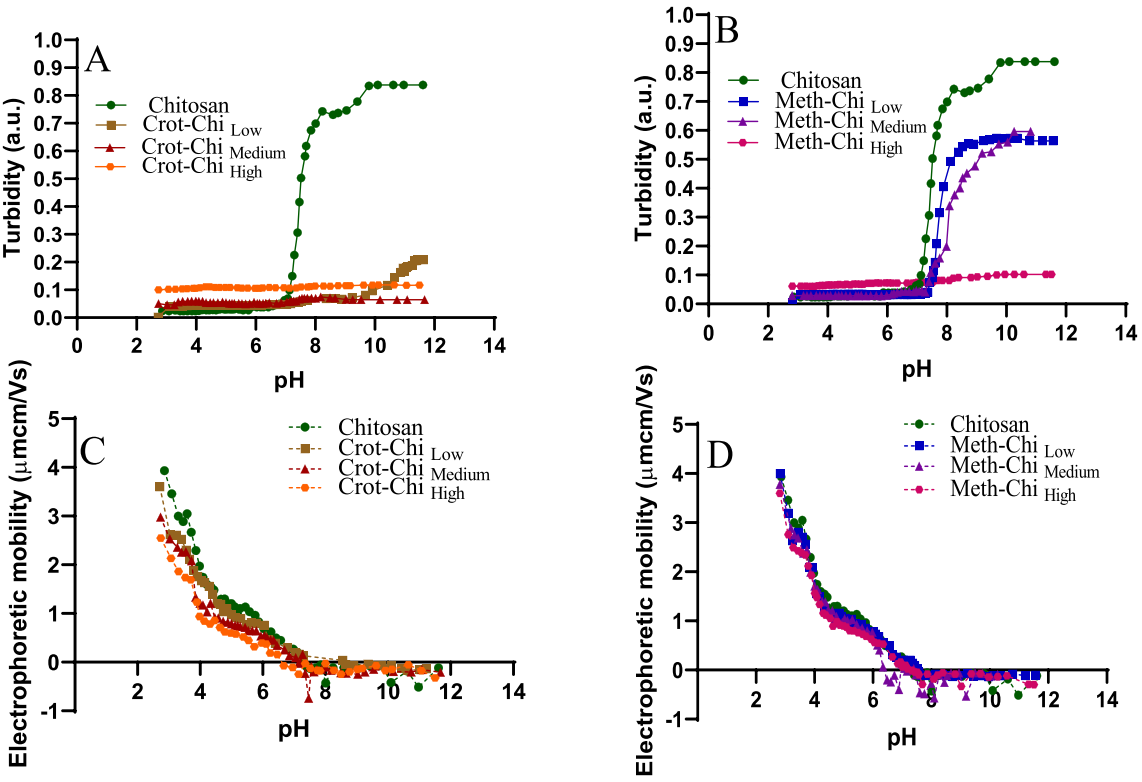

Fig. 4. Effect of pH on turbidity (A and B) and electrophoretic mobility (C and D) of chitosan and its crotonoylated (A, C) and methacryloylated (B, D) derivatives in aqueous solutions. All polymeric solutions were prepared in 3 % acetic acid.

Conventional nasal sprays have a typical median particle size between 30 and 120 μm. Droplets larger than this tend to deposit at the front of the nose, therefore particle size is crucial for nasal drug delivery [42].

In this study, chitosan and its derivatives were used to prepare microparticles using spray-drying technique which plays a key role in pharmaceutical research and development [43]. These particles were characterised using laser diffraction and digital microscopy techniques. Fig. 5**A and B** presents particle size distributions and images of

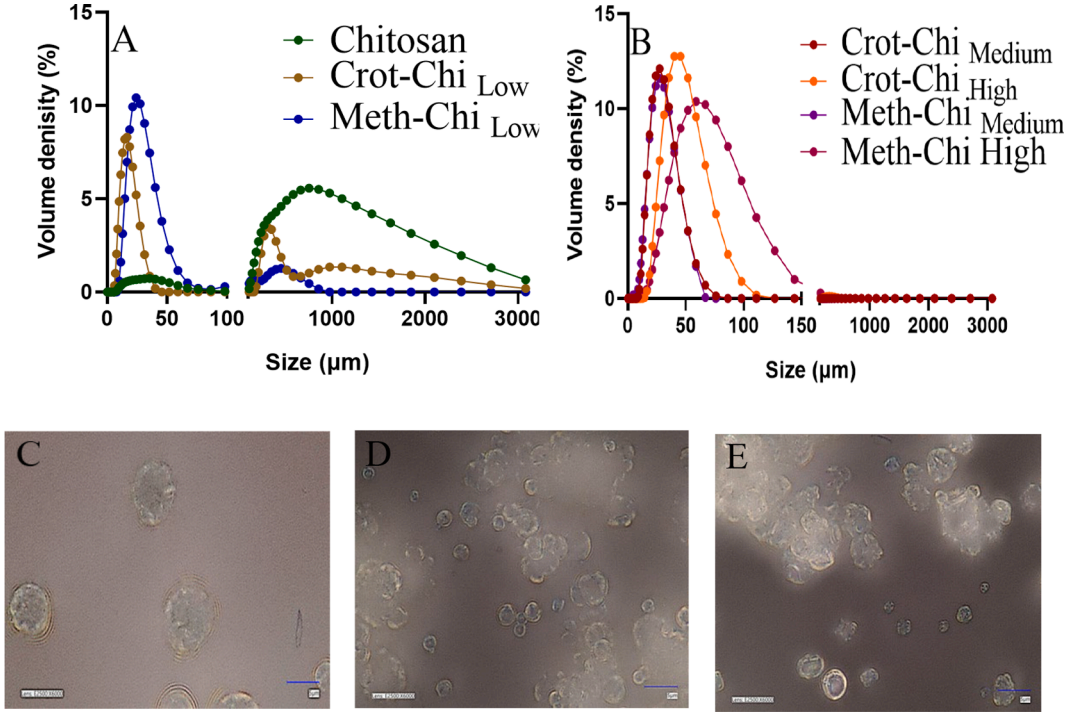

Fig. 5. Laser diffraction data and exemplar images of digital microscopy of spray dried powders. Wet dispersion laser diffraction data for chitosan and low modified crotonoloylated and methacryloylated chitosan (A) for medium and high modified crotonoylated and methacryloylated chitosan (B). Digital microscopy image of chitosan (C), dry microparticles Crot-Chi $_{Medium}$ microparticles (D) and Meth-Chi $_{Medium}$ microparticles at 6000 × magnification. Scale bar is 5 μm.

individual particles. Wet dispersion laser diffraction revealed that some samples displayed polymodal particle size distributions, with parent chitosan particles displaying the presence of two size populations (10 to 100 μm and 100 to 3080 μm). Similar polymodal size distributions were observed for the particles generated from chitosan with the lowest degrees of crotonylation (18.1 %) and methacryloylation (8.4 %). This is possibly related to the presence of numerous hydroxyl and amino groups in chitosan. These groups present on the surface of microparticles may form interparticle hydrogen bonds leading to their stronger aggregation. In this case the two populations in size distributions correspond to individual particles and their aggregates. The microparticles generated from chitosan derivatives with medium and high crotonylation and methacryloylation degrees display monomodal size distributions and this is likely due to the reduced ability of interparticle binding via H bonds.

The mean particle size and span values for all formulations are summarised in Table 3. Span is a measure of width of particle size distribution and is calculated using the formula [D90 – D10]/[D50] [44]. Parent chitosan particles had the largest size (833 μm) and span compared to the modified derivatives. Crot-Chi $_{Low}$ and Meth-Chi $_{Low}$ had the biggest particle size and span of the modified derivatives.

Evaluation of the microparticles using digital microscopy provided substantially smaller size values for all the studied microparticles compared to the data generated using laser diffraction (Fig. 5**D,E** and Table 3). This discrepancy could be attributed to two factors. Firstly, while direct imaging measures the sizes of individual particles, laser diffraction results are influenced by particle aggregation. Secondly, in microscopy experiments, the particles were examined in a dry state. Conversely, during laser diffraction, the particles were dispersed in deionised water, which could cause them to swell and thus appear larger. Anyways, the particle sizes measured using microscopy in dry state have shown the following trend: particles made from parent chitosan and low modified derivatives have a higher size compared to medium and high modified derivatives. Medium modified derivatives displayed lowest particle size. The particle sizes measured using microscopy in the dry state exhibited the following trend: particles made from parent chitosan and low-modified derivatives had larger particle sizes compared to medium- and high-modified derivatives. Notably, the medium-modified derivatives displayed the smallest particle sizes.

3.6. Mucoadhesion

Spray dried microparticles were used to study the mucoadhesive properties by evaluating their detachment from freshly excised sheep nasal tissue ex vivo using a tensile method. The microparticles were attached to the probe by a glue dot, the probe arm was lowered and was in contact with the nasal tissue. The withdrawal of the probe provides a detachment profile giving information about two characteristics of mucoadhesion. The area under the detachment curve provides the total work of adhesion (W_{adh}) and the maximum value on this curve gives the peak force of detachment (F_{det}).

Table 3
Particle size measurement from laser diffraction and digital microscopy.

Sample	Average particle size Laser diffraction(μm)	Span	Digital microscopy particle size (μm)
Chitosan	833	2.58	5.66 ± 1.41
Crot-Chi $_{Low}$	259	2.48	2.73 ± 1.18
Crot-Chi $_{Medium}$	31	1.09	2.32 ± 0.84
Crot-Chi $_{High}$	50	1.02	3.59 ± 1.32
Meth-Chi $_{Low}$	77	1.26	3.13 ± 1.49
Meth-Chi $_{Medium}$	30	1.12	2.59 ± 0.59
Meth-Chi $_{High}$	65	0.93	3.10 ± 1.16

Fig. 6 shows the values of peak force of detachment and total work of adhesion recorded for microparticles prepared from chitosan and its derivatives plotted as a function of their degree of substitution. The value for degree of substitution at zero represents particles of unmodified chitosan. Chitosan is known to have excellent mucoadhesive properties as reported in literature [8,45]. The values of the total work of adhesion and maximal force of detachment of particles derived from both crotonoloylated and methacryloylated derivatives are higher than that of parent chitosan. This indicates that both types of chitosan derivatisation result in improvement of its mucoadhesive properties. It should be noted that methacryloylated derivatives do not show any significant difference from crotonoylated chitosan based on the peak force of detachment results; however, the sample of methacryloylated chitosan$_{medium}$ displays statistically significant superior $W_{adh} = 0.282 \pm 0.087$ N·mm compared to the particles of crotonoloylated chitosan$_{medium}$ with comparable degree of substitution ($W_{adh} = 0.180 \pm 0.067$ N·mm). Mucoadhesive properties of chitosan are predominantly due to the electrostatic interactions between the positively charged amino-groups and the negatively charged carboxylic and sulphate groups in mucins. However, the hydroxyl groups of chitosan can also be involved in hydrogen bonding as well. The introduction of methacryloylated and crotonoloylated groups into the chitosan backbone may reduce the contribution of electrostatic interactions. Nevertheless, the unsaturated bonds present in chitosan's derivatives can covalently bind to the thiol groups present in mucins. The degree of substitution plays an important role in this interaction sustaining the mucoadhesive properties [46]. Fig. 6**B** shows that the total work of adhesion initially increases with the degree of substitution until it reaches a maximum; then a decrease in adhesiveness is observed. This can be attributed to reduction in the contribution of electrostatic interactions as the concentration of positively charged amino groups is reduced with modification of chitosan. Furthermore, steric hindrance due to the bulkiness of introduced groups can also contribute to a decrease in mucoadhesive properties [47].

3.7. Wash-off studies

To evaluate the retention of chitosan and its derivatives on the sheep nasal mucosa, polymeric solutions with 0.1 % sodium fluorescein were spray dried to produce microparticles. These microparticles were dispersed in ANF and placed on the tissue and washed off to study the retention. Fig. 7 shows the fluorescent images of the microparticles on nasal mucosa at different time points when washed with ANF. ImageJ software was used to analyse these images. Similarly to tensile strength measurements, crotonoloylated chitosan$_{medium}$ and methacryloylated chitosan$_{medium}$ exhibited greater retention on the mucosa compared to chitosan consistently from 20 min of starting the wash-off (Fig. 8). This improved retention can be attributed to the ability of methacryloylated and crotonoylated groups to bind covalently to the thiol groups present in cysteine rich domains in mucin [48]. This improvement in retention can potentially lead to improved drug bioavailability at site of action. The results of the retention study confirm that modifying chitosan with methacryloylated and crotonoylated groups does improve the mucoadhesive properties; therefore, these chemical modifications of chitosan can be used as potential mucoadhesive drug carriers.

WO_{50} values were calculated from wash off profiles to provide a further characterisation of the mucoadhesive properties of these formulations (**Figure S3**). WO_{50} values provide an opportunity for a direct comparison between chitosan derivatives differing in their degrees of substitution. The time points were converted into volume (mL) based on the rate of ANF used for washing off (0.5 mL/min). Fig. 9 illustrates the relationship between WO_{50} values and the degree of substitution in chitosan derivatives. At lower degrees of substitution, methacryloylated chitosan demonstrates a higher retention capacity on the mucosa. Nevertheless, a particular sample of crotonoylated chitosan, with a degree of substitution of 26.1 %, surpasses this retention performance, indicating even greater efficacy in mucosal retention. Nevertheless, a

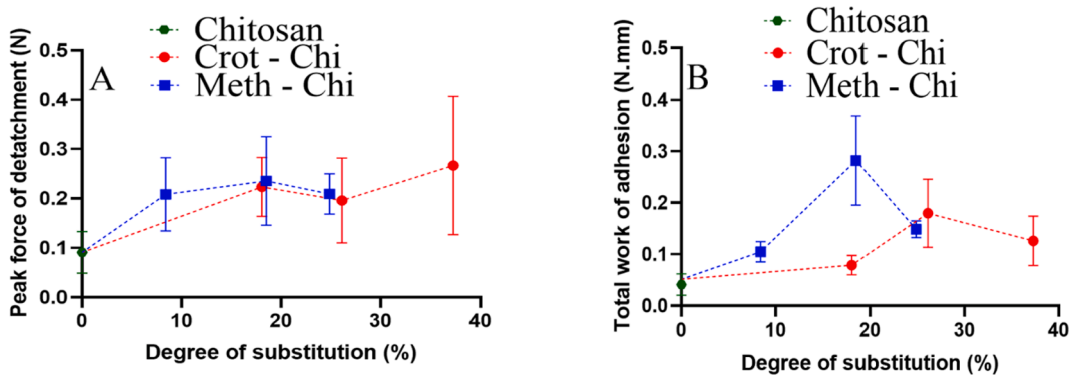

Fig. 6. Mucoadhesion characteristics of spray dried microparticles at different degrees of substitution. Maximal detachment force (A) and total work of adhesion (B). Data shows the mean value and standard deviation (n = 9).

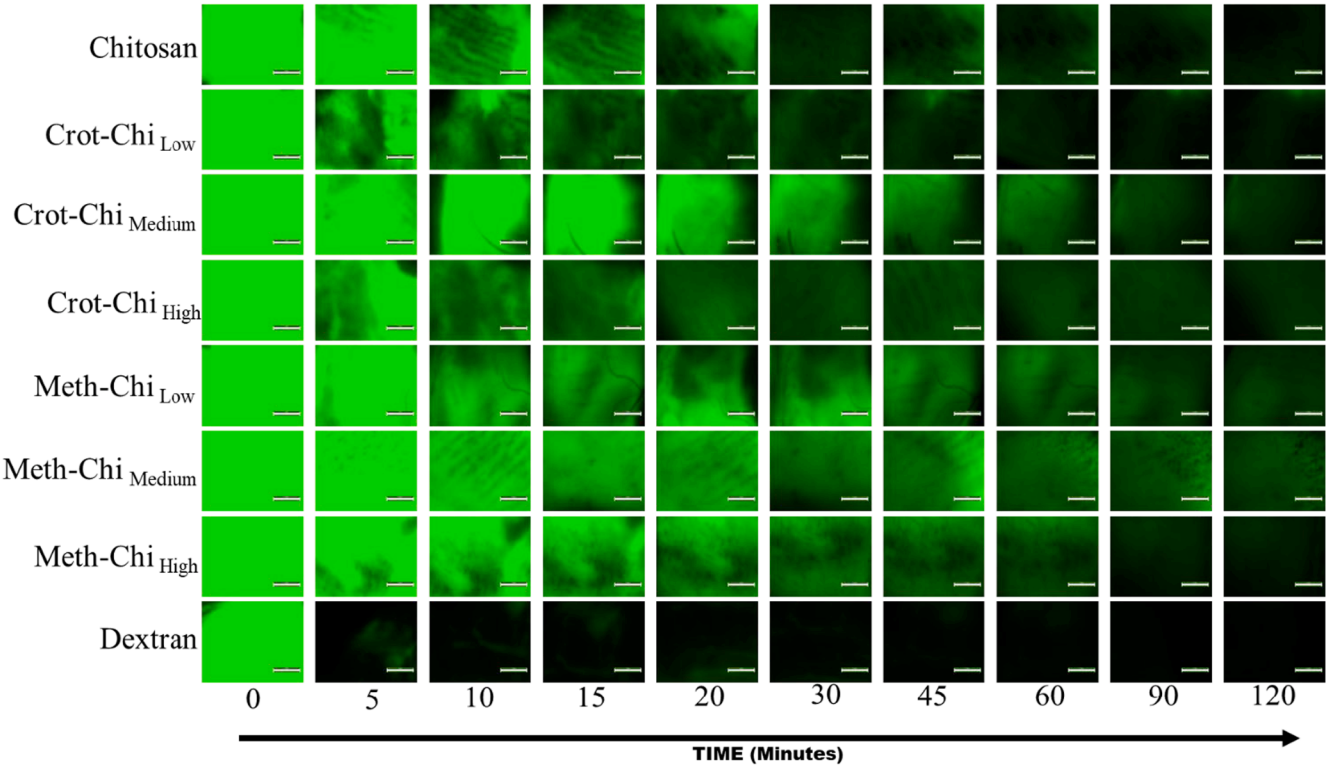

Fig. 7. Exemplar fluorescence images showing retention of spray dried chitosan and its derivatives on sheep nasal mucosa washed with ANF at 0.5 mL/min at different time points. Scale bar is 2 mm.

further increase in the degree of substitution of crotonylated chitosan to 37.3 % results in a dramatic reduction of its mucoadhesive properties. This is likely to be due to its less cationic nature.

3.8. Acute toxicity

Planaria are freshwater flatworms that have emerged as an excellent model organism for pharmacological and toxicological research [49]. Recently, we have adapted the use planaria for assessment of irritant properties of chemicals using several approaches [26]. One approach is to evaluate the acute toxicity of chemicals in planaria. This involves exposing live worms to aqueous solutions of these chemicals for varying periods and assessing whether the treatment results in their death. In this study, the acute toxicity assay revealed that 0.1 % w/v solutions of chitosan and its derivatives at different pH values (6.0, 6.2, 6.4, 6.6, 6.8) in water and in APW do not cause death in planaria for 24, 48 and 72 h of exposure. After each 24 h cycle, planaria were moved to APW solution to check their movement (**Figure S4**). This toxicological study under different pH conditions highlighted that planaria can survive in a wider pH range than previously reported in literature [50,51]. Planaria in APW at different pHs was used as a negative control along with 1 % w/v benzalkonium chloride (BAC) prepared in APW as a positive control. All the planaria survived except those exposed to 1 % w/v BAC, which resulted in dead worms with no signs of movement.

3.9. Planarian toxicity fluorescent assay

The Khutoryanskiy group previously developed a new fluorescent assay using live planaria (**Figure S5**) to evaluate the effects of chemicals on planarian body wall integrity and barrier function [26]. In this assay, live planaria are first exposed to solutions of the chemicals being tested for irritant properties. After this exposure, the worms are immersed in a solution of sodium fluorescein. If the chemicals have irritant properties, they will damage the planarian epithelia, making them more permeable

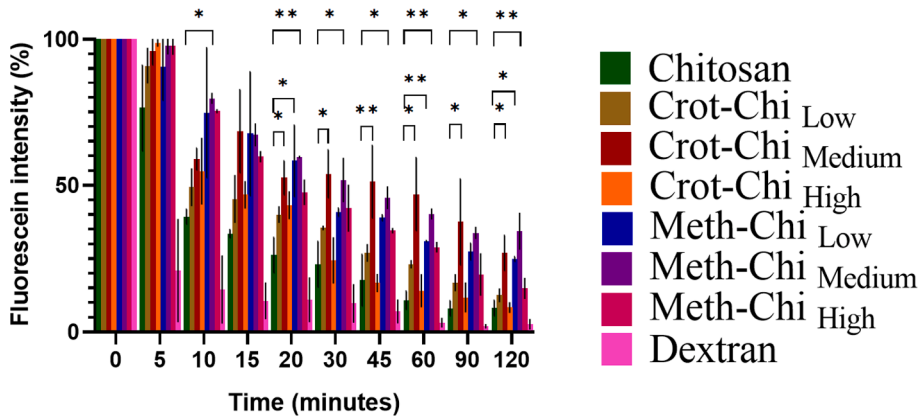

Fig. 8. Retention of chitosan and its derivatives on sheep nasal mucosa after washing with ANF at 0.5 mL/min at different time points. Data is expressed as mean ± standard deviation (n = 3). Statistical significance was determined using one way ANOVA and significant differences are shown with * when $p < 0.05$ and ** when $p < 0.005$.

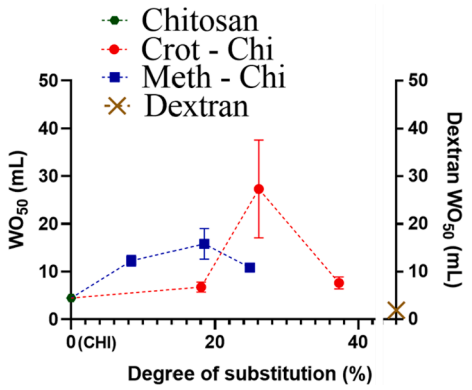

Fig. 9. WO_{50} results for the retention of microparticles on the mucosa as a function of chitosan's degree of substitution. Dextran was used as a negative control. Error bars represent standard deviation (n = 3).

to the fluorescent dye. This increased permeability allows the dye to penetrate the worm bodies, which is visible under fluorescent microscopy. The extent of dye penetration is then assessed using ImageJ to provide quantitative information. In this study, live planaria were subjected to 0.1 % w/v solutions of chitosan and its derivatives and to 1 % w/v solution of BAC at different pH values. The results of these experiments are presented in Fig. 10. An exposure of planaria to crotonoloylated and methacryloylated chitosan solutions for 24 h did not reveal any statistically significant reduction in the epithelial barrier function compared to unmodified chitosan ($p > 0.05$). This result indicates that the novel polymers bearing crotonyl and methacryloyl functional groups do not exhibit any irritation properties similarly to parent chitosan. However, when planaria were exposed to strongly irritant 1 % w/v BAC solution used as a positive control for just 1 h, statistically significant increase in the fluorescence intensity was observed due to enhanced penetration of sodium fluorescein into their body.

3.10. Cell toxicity

The cell toxicity of chitosan and its derivatives was also evaluated using *in vitro* MTT assay on a human intestinal Caco-2 cell line. This cell line is widely utilised as a model to simulate mucosal epithelia and is characterised by the formation of tight junctions, as well as a well-differentiated brush border [52,53]. Generally, the use of MTT assay for cell viability is based on their metabolic activity – the conversion of MTT to insoluble formazan crystals. Fig. 11 shows the effect of chitosan and its derivatives on Caco-2 cell monolayers after 4 and 24 h of exposure. Approximately 69 ± 6 %, 70 ± 4 %, and 70 ± 11 % of cell viability were observed for chitosan at concentrations 0.01, 0.05 and 0.1 mg/mL after 4 h exposure, respectively. This value is very close to the threshold set by the International Organisation for Standardisation (ISO) 10993-5 guidelines for *in vitro* cytotoxicity tests [54], which considers viability >70 % as non-cytotoxic. Previous studies [45,52] indicated that the CaCo-2 cell viability for chitosan solutions at pH 6.3 and a concentration of 0.5 mg/mL after 4 h was approximately 100 %. In our case, the differences in the viability are likely related to the combination of several factors, such as the type of chitosan, its purity, pH, and cell density [55].

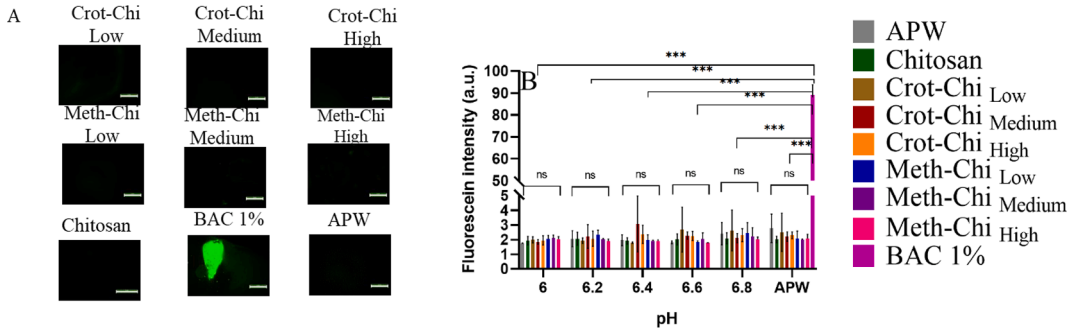

Fig. 10. Planarian toxicity fluorescent assay. Exemplar fluorescent images (scale bar is 2 mm) (A) and fluorescence intensity values calculated using ImageJ analysis of fluorescent images, following 24 h exposure of planaria to 0.1 % w/v solutions of chitosan, its derivatives and 1 % w/v BAC, with subsequent immersion of the worms in 0.1 % w/v sodium fluorescein (B). Each experiment was performed using 3 different worms (n = 3) and mean fluorescence intensity values ± standard deviations were calculated. Statistical significance was determined using one way ANOVA and significant differences are shown with * when $p < 0.05$, ** when $p < 0.005$ and *** when $p < 0.0005$.

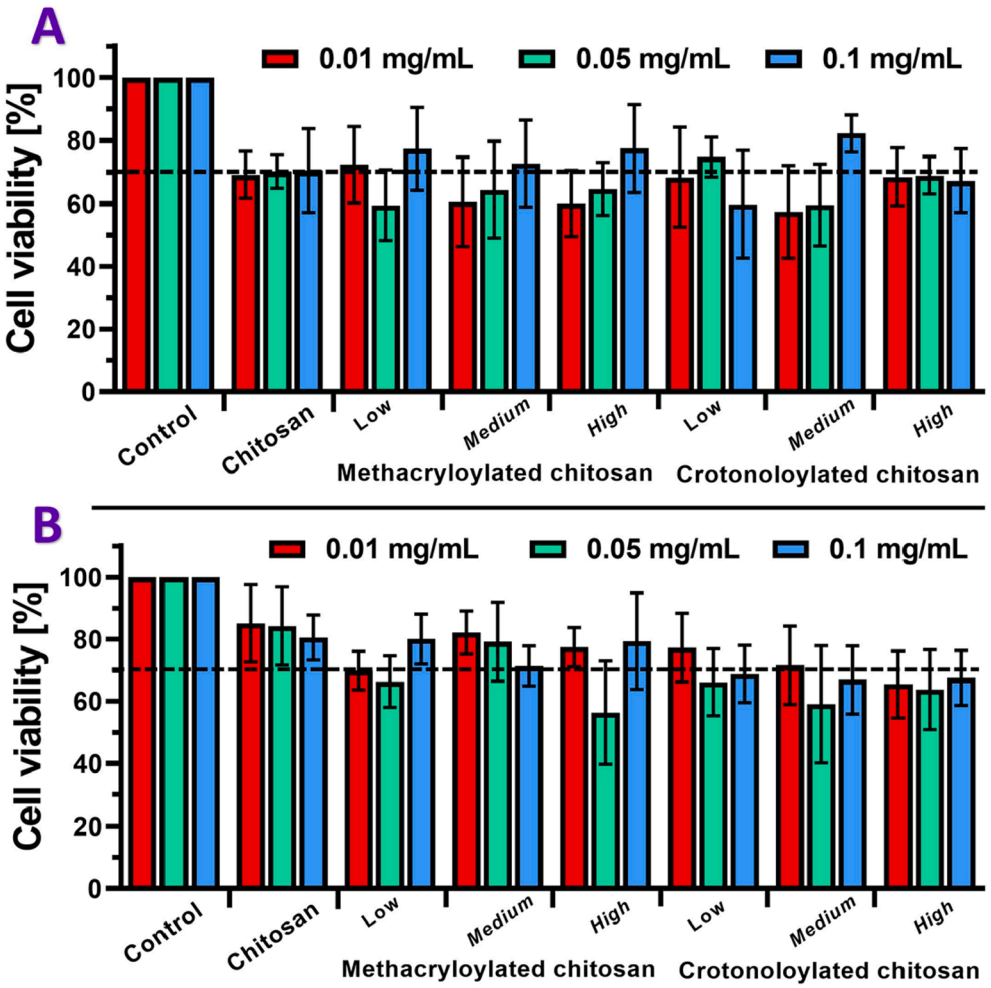

Fig. 11. Viability of Caco-2 cells assessed after exposure to 0.01, 0.05, and 0.1 mg/mL solutions of chitosan and its derivatives for 4 h (A) and 24 h (B), as determined by the MTT assay. Statistical significance was determined using one way ANOVA and significant differences are shown with * when $p < 0.05$, ** when $p < 0.005$ and *** when $p < 0.0005$.

The toxicity of chitosan in contrast with the crotonoloylated and methacryloylated derivatives showed no statistically significant difference in all ranges of concentrations. Similar effects were also observed in the study of Kolawole et al. [20], where the toxicity of chitosan and methacrylated chitosan was evaluated in UMUC3 cell line. Moreover, their report also demonstrated the close levels of cell viability after 4 h in the concentration range between 0.05 and 0.1 mg/mL. In our case, there were also no statistically significant differences between chitosan and its derivatives after 24 h. Thus, the toxicity of crotonoloylated and methacryloylated chitosan *in vitro* is very similar to the parent chitosan. Therefore, these new chitosan derivatives could potentially be used as mucoadhesive excipients in drug delivery.

4. Conclusions

This study demonstrated that modification of chitosan with methacryloyl and crotonoyl moieties results in polymers with substantially improved mucoadhesive properties. This modification can be achieved through single-stage reactions of chitosan with methacrylic and crotonic anhydrides. The physicochemical properties of these new derivatives are dependent on the degree of substitution of chitosan with these unsaturated groups. Both crotonoylated and methacryloylated chitosan demonstrated that an initial increase in the degree of substitution enhances mucoadhesive properties and solubility. This is due to the ability of unsaturated groups to form covalent bonds with thiols present in mucins via 1,2-Michael addition reactions happening under physiological conditions. However, highly substituted polymers become partially soluble and less mucoadhesive due to the slightly hydrophobic nature of these functional groups. The introduction of crotonoyl and methacryloyl groups into these polymers does not negatively impact their toxicological profile, as evaluated using an *in vivo* planaria model and an *in vitro* cell culture assay with Caco-2 cells. These new chitosan derivatives can be considered as new excipients for formulation of mucoadhesive dosage forms for transmucosal drug delivery.

CRediT authorship contribution statement

Shiva Vanukuru: Writing – original draft, Methodology, Investigation, Formal analysis. **Fraser Steele:** Resources. **Natalia N. Porfiryeva:** Investigation. **Alejandro Sosnik:** Resources. **Vitaliy V. Khutoryanskiy:** Writing – review & editing, Supervision, Resources, Project administration, Conceptualization.

Declaration of competing interest

The authors declare that they have no known competing financial interests or personal relationships that could have appeared to influence the work reported in this paper.

Acknowledgments

The authors gratefully acknowledge technical services staff within

the Chemical Analysis Facility at the University of Reading for technical support and assistance in this work. We also acknowledge Mr Kristian Gregory from Keyence Microscopy division for technical help with imaging microparticles. V.V.K. acknowledges the financial support provided by the Royal Society for his Industry Fellowship (IF/R2/222031). A.S. thanks the support of the Tamara and Harry Handelsman Academic Chair.

Appendix A. Supplementary material

Supplementary data to this article can be found online at https://doi.org/10.1016/j.ejpb.2024.114575.

Data availability

Data will be made available on request.

References

[1] R. Shaikh, T. Raj Singh, M. Garland, A. Woolfson, R. Donnelly, Mucoadhesive drug delivery systems, J. Pharm. Bioallied Sci. (2011).
[2] J.K.W. Lam, C.C.K. Cheung, M.Y.T. Chow, E. Harrop, S. Lapwood, S.I.G. Barclay, et al., Transmucosal drug administration as an alternative route in palliative and end-of-life care during the COVID-19 pandemic, Advanced Drug Delivery Reviews 160 (2020) 234–243.
[3] T.M.M. Ways, W.M. Lau, V.V. Khutoryanskiy, Chitosan and its derivatives for application in mucoadhesive drug delivery systems, Polymers (Basel) 10 (3) (2018).
[4] S. Mansuri, P. Kesharwani, K. Jain, R.K. Tekade, N.K. Jain, Mucoadhesion: A promising approach in drug delivery system, React. Funct. Polym. 100 (2016) 151–172, https://doi.org/10.1016/j.reactfunctpolym.2016.01.011.
[5] R.J. Robinson, M.A. Longer, M. Veillard, Bioadhesive polymers for controlled drug delivery, Ann N Y Acad Sci. (1987).
[6] V.V. Khutoryanskiy, Advances in mucoadhesion and mucoadhesive polymers, Macromol Biosci. 11 (6) (2011) 748–764.
[7] S. Şenel, S.J. McClure, Potential applications of chitosan in veterinary medicine, Adv Drug Deliv Rev. 56 (10) (2004) 1467–1480.
[8] I.A. Sogias, A.C. Williams, V.V. Khutoryanskiy, Why is chitosan mucoadhesive? Biomacromolecules 9 (7) (2008) 1837–1842.
[9] S.S. Davis, L. Illum, Absorption enhancers for nasal drug delivery, Clin. Pharmacokinet. 42 (13) (2003) 1107–1128.
[10] S.C. Baos, D.B. Phillips, L. Wildling, T.J. McMaster, M. Berry, Distribution of sialic acids on mucins and gels: A defense mechanism, Biophys J. 102 (1) (2012) 176–184.
[11] C. Palazzo, G. Trapani, G. Ponchel, A. Trapani, C. Vauthier, Mucoadhesive properties of low molecular weight chitosan- or glycol chitosan- and corresponding thiomer-coated poly(isobutylcyanoacrylate) core-shell nanoparticles, Eur. J. Pharm. Biopharm. 117 (2017) 315–323.
[12] I.A. Sogias, V.V. Khutoryanskiy, A.C. Williams, Exploring the factors affecting the solubility of chitosan in water, Macromol. Chem. Phys. 211 (4) (2010) 426–433.
[13] I. Aranaz, A.R. Alcántara, M.C. Civera, C. Arias, B. Elorza, A.H. Caballero, et al., Chitosan: An overview of its properties and applications, Polymers (Basel) 13 (19) (2021).
[14] Q. Chen, Y. Qi, Y. Jiang, W. Quan, H. Luo, K. Wu, et al., Progress in research of chitosan chemical modification technologies and their applications, Mar Drugs. 20 (8) (2022).
[15] A. Bernkop-Schnürch, Thiomers: A new generation of mucoadhesive polymers, Adv. Drug. Deliv. Rev. 57 (11) (2005) 1569–1582.
[16] P. Tonglairoum, R.P. Brannigan, P. Opanasopit, V.V. Khutoryanskiy, Maleimide-bearing nanogels as novel mucoadhesive materials for drug delivery, J. Mater. Chem. B. 4 (40) (2016) 6581–6587.
[17] F. Buang, A. Chatzifragkou, M.C.I.M. Amin, V.V. Khutoryanskiy, Synthesis of methacryloylated hydroxyethylcellulose and development of mucoadhesive wafers for buccal drug delivery, Polymers (Basel) 15 (1) (2022).
[18] A. Štorha, E.A. Mun, V.V. Khutoryanskiy, Synthesis of thiolated and acrylated nanoparticles using thiol-ene click chemistry: Towards novel mucoadhesive materials for drug delivery, RSC Adv. 3 (30) (2013) 12275–12279.
[19] M. Ouellette, F. Masse, M. Lefebvre-Demers, Q. Maestracci, P. Grenier, R. Millar, et al., Insights into gold nanoparticles as a mucoadhesive system, Sci. Rep. 8 (1) (2018) 1–15.
[20] O.M. Kolawole, W.M. Lau, V.V. Khutoryanskiy, Methacrylated chitosan as a polymer with enhanced mucoadhesive properties for transmucosal drug delivery, Int. J. Pharm. 550 (1–2) (2018) 123–129.
[21] A.A. Cockram, T.J. Neal, M.J. Derry, O.O. Mykhaylyk, N.S.J. Williams, M. W. Murray, et al., Effect of monomer solubility on the evolution of copolymer morphology during polymerization-induced self-assembly in aqueous solution, Macromolecules 50 (3) (2017) 796–802.
[22] T. Hibbard, H. Mitchell, Y. Kim, K. Shankland, H. Al-Obaidi, Spray dried progesterone formulations for carrier free dry powder inhalation, Eur. J. Pharm. Biopharm. 189 (2023) 264–275, https://doi.org/10.1016/j.ejpb.2023.06.018.
[23] X. Shan, S. Aspinall, D.B. Kaldybekov, F. Buang, A.C. Williams, V.V. Khutoryanskiy, Synthesis and evaluation of methacrylated poly(2-ethyl-2-oxazoline) as a mucoadhesive polymer for nasal drug delivery, ACS Appl. Polym. Mater. 3 (11) (2021) 5882–5892.
[24] M. Fu, S.K. Filippov, A.C. Williams, V.V. Khutoryanskiy, On the mucoadhesive properties of synthetic and natural polyampholytes, J. Colloid Interf. Sci. 659 (2024) 849–858, https://doi.org/10.1016/j.jcis.2023.12.176.
[25] D.B. Kaldybekov, S.K. Filippov, A. Radulescu, V.V. Khutoryanskiy, Maleimide-functionalised PLGA-PEG nanoparticles as mucoadhesive carriers for intravesical drug delivery, Eur. J. Pharm. Biopharm. 143 (2019) 24–34, https://doi.org/10.1016/j.ejpb.2019.08.007.
[26] S.I. Shah, A.C. Williams, W.M. Lau, V.V. Khutoryanskiy, Planarian toxicity fluorescent assay: A rapid and cheap pre-screening tool for potential skin irritants, Toxicol. Vitr. 69 (2020), https://doi.org/10.1016/j.tiv.2020.105004.
[27] W. Tan, Q. Li, F. Dong, J. Zhang, F. Luan, L. Wei, et al., Novel cationic chitosan derivative bearing 1,2,3-triazolium and pyridinium: synthesis, characterization, and antifungal property, Carbohydr. Polym. 182 (2018) 180–187.
[28] Y. Cao, Y.F. Tan, Y.S. Wong, M. Aminuddin, B. Ramya, M.W.J. Liew, et al., Designing siRNA/chitosan-methacrylate complex nanolipogel for prolonged gene silencing effects, Sci. Rep. 12 (1) (2022) 1–14, https://doi.org/10.1038/s41598-022-07554-0.
[29] L. Zhu, K.M. Bratlie, pH sensitive methacrylated chitosan hydrogels with tunable physical and chemical properties, Biochem. Eng. J. 132 (2018) 38–46, https://doi.org/10.1016/j.bej.2017.12.012.
[30] M.L. Tummino, G. Magnacca, D. Cimino, E. Laurenti, R. Nisticò, The innovation comes from the sea: Chitosan and alginate hybrid gels and films as sustainable materials for wastewater remediation, Int. J. Mol. Sci. 21 (2) (2020) 1–16.
[31] A. Pawlak, M. Mucha, Thermogravimetric and FTIR studies of chitosan blends, Thermochim Acta. 396 (1–2) (2003) 153–166.
[32] S.M. Saraiva, S.P. Miguel, M.P. Ribeiro, P. Coutinho, I.J. Correia, Synthesis and characterization of a photocrosslinkable chitosan-gelatin hydrogel aimed for tissue regeneration, RSC Adv. 5 (78) (2015) 63478–63488.
[33] R.R. Jalal, T.M.M. Ways, M.H. Abu Elella, D.A. Hassan, V.V. Khutoryanskiy, Preparation of mucoadhesive methacrylated chitosan nanoparticles for delivery of ciprofloxacin, Int. J. Biol. Macromol. 242 (P4) (2023), https://doi.org/10.1016/j.ijbiomac.2023.124980.
[34] D. Lupa, W. Płaziński, A. Michna, M. Wasilewska, P. Pomastowski, A. Gołębiowski, et al., Chitosan characteristics in electrolyte solutions: combined molecular dynamics modeling and slender body hydrodynamics, Carbohydr. Polym. 292 (2022).
[35] S.H. Chang, H.T.V. Lin, G.J. Wu, G.J. Tsai, pH Effects on solubility, zeta potential, and correlation between antibacterial activity and molecular weight of chitosan, Carbohydr. Polym. 134 (2015) 74–81.
[36] N. Saïed, M. Aider, Zeta potential and turbidimetry analyzes for the evaluation of chitosan/phytic acid complex formation, J. Food Res. 3 (2) (2014) 71.
[37] L. Casettari, L. Illum, Chitosan in nasal delivery systems for therapeutic drugs, J. Control Release. 190 (2014) 189–200, https://doi.org/10.1016/j.jconrel.2014.05.003.
[38] R. Awad, A. Avital, A. Sosnik, Polymeric nanocarriers for nose-to-brain drug delivery in neurodegenerative diseases and neurodevelopmental disorders, Acta Pharm. Sin. B. 13 (5) (2023) 1866–1886, https://doi.org/10.1016/j.apsb.2022.07.003.
[39] J. Tai, M. Han, D. Lee, I.H. Park, S.H. Lee, T.H. Kim, Different methods and formulations of drugs and vaccines for nasal administration, Pharmaceutics. 14 (5) (2022) 1–19.
[40] L.A. Keller, O. Merkel, A. Popp, Intranasal drug delivery: opportunities and toxicologic challenges during drug development, Drug Deliv. Transl. Res. 12 (4) (2022) 735–757, https://doi.org/10.1007/s13346-020-00891-5.
[41] S. Bahadur, D.M. Pardhi, J. Rautio, J.M. Rosenholm, K. Pathak, Intranasal nanoemulsions for direct nose-to-brain delivery of actives for cns disorders, Pharmaceutics 12 (2020) 1–27.
[42] S.S. Sangolkar, V.S. Adhao, D.G. Mundhe, H.S. Sawarkar, Particle size determination of nasal drug delivery system: A review, Int. J. Pharm. Sci. Rev. Res. 17 (1) (2012) 66–73.
[43] A. Sosnik, K.P. Seremeta, Advantages and challenges of the spray-drying technology for the production of pure drug particles and drug-loaded polymeric carriers, Adv. Colloid Interf. Sci. 223 (2015) 40–54.
[44] M. Ortiz, D.S. Jornada, A.R. Pohlmann, S.S. Guterres, Development of novel chitosan microcapsules for pulmonary delivery of dapsone: characterization, aerosol performance, and in vivo toxicity evaluation, AAPS Pharm. Sci. Tech. 16 (5) (2015) 1033–1040.
[45] J.D. Smart, The basics and underlying mechanisms of mucoadhesion, Adv. Drug Deliv. Rev. 57 (11) (2005) 1556–1568.
[46] M.K. Amin, J.S. Boateng, Enhancing stability and mucoadhesive properties of chitosan nanoparticles by surface modification with sodium alginate and polyethylene glycol for potential oral mucosa vaccine delivery, Mar. Drugs. 20 (3) (2022) 1–22.
[47] E.M.A. Hejjaji, A.M. Smith, G.A. Morris, Evaluation of the mucoadhesive properties of chitosan nanoparticles prepared using different chitosan to tripolyphosphate (CS:TPP) ratios, Int. J. Biol. Macromol. 120 (2018) 1610–1617, https://doi.org/10.1016/j.ijbiomac.2018.09.185.
[48] K. Mfoafo, R. Mittal, A. Eshraghi, Y. Omidi, H. Omidian, Thiolated polymers: An overview of mucoadhesive properties and their potential in drug delivery via mucosal tissues, J. Drug Deliv. Sci. Technol. 85 (2023), https://doi.org/10.1016/j.jddst.2023.104596.

[49] D. Hagstrom, O. Cochet-Escartin, S. Zhang, C. Khuu, E.M.S. Collins, Freshwater planarians as an alternative animal model for neurotoxicology, Toxicol. Sci. 147 (1) (2015) 270–285.
[50] A.H. Harrath, M. Charni, R. Sluys, F. Zghal, S. Tekaya, Ecology and distribution of the freshwater planarian schmidtea mediterranea in tunisia, Ital. J. Zool. 71 (3) (2004) 233–236.
[51] M.R.P. Dean, E.M. Duncan, Laboratory maintenance and propagation of freshwater planarians, Curr. Protoc. Microbiol. 59 (1) (2020) 1–20.
[52] N.J. Darling, C.L. Mobbs, A.L. González-Hau, M. Freer, S. Przyborski, Bioengineering novel in vitro Co-culture models that represent the human intestinal mucosa with improved Caco-2 structure and barrier function, Front. Bioeng. Biotechnol. 8 (2020) 1–15.
[53] V. Meunier, M. Bourrié, Y. Berger, G. Fabre, The human intestinal epithelial cell line Caco-2; pharmacological and pharmacokinetic applications, Cell Biol. Toxicol. 11 (3–4) (1995) 187–194.
[54] Internationational organisation for standardization. ISO 10993−5: Biological evaluation of medical devices_Part 5: Tests for in vitro cytotoxicity. . 2009. Available from: https://www.iso.org/obp/ui/#iso:std:iso:10993:-5:ed-3:v1:en.
[55] M. Kus, I. Ibragimow, H. Piotrowska-Kempisty, Caco-2 cell line standardization with pharmaceutical requirements and in vitro model suitability for permeability assays, Pharmaceutics. 15 (11) (2023).